An Investigation of the Effects of Austenite Strength and Austenite Stacking Fault Energy on the Morphology of Martensite in Fe-Ni-Cr-0.3C Alloys

M. J. CARR, J. R. STRIFE, AND G. S. ANSELL

The relative effects of austenite stacking fault energy and austenite yield strength on martensite morphology have been investigated in a series of three Fe-Ni-Cr-C alloys. Carbon content (0.3 wt pct) and M_S temperature (−15°C) were held constant within the series. Austenite yield strength at M_S was measured by extrapolating elevated temperature tensile data. Austenite stacking fault energy was measured by the dislocation node technique. Martensite morphologies were characterized by transmission electron microscopy and electron diffraction techniques. A transition from plate to lath martensite occurred with decreasing austenite stacking fault energy. The austenite yield strength at M_S for the low SFE, lath-forming alloy was found to be higher than previously reported for lath-forming alloys. The relative effects of these variables on martensite morphologies in these alloys is discussed.

FERROUS martensite forms from austenite by a diffusionless, shear-type transformation. The product phase is not unique, however, and several morphologies have been identified in steels. These morphologies are generally divided into three types: lath martensite, typically formed as packets of sheets or heavily dislocated, bcc, untwinned, needle-like units; plate martensite, typically formed as individual bct plates containing many fine twins; and epsilon martensite, an hcp phase.

Many previous investigations have sought to determine which variables control the morphology of the martensite that forms in a given steel. Variables reported to affect morphology include: M_S temperature,[1-4] substitutional solute content,[1,2,5-8] interstitial solute content,[1,2-9] austenite shear strength,[8,10-12] austenite stacking fault energy,[13-16] quench rate above M_S,[15] thermomechanical processing,[18] and hydrostatic pressure.[19] Some of these are of a secondary nature, and the factors controlling martensite morphology are usually reduced to one or a combination of the following: M_S temperature, carbon content, austenite yield strength, and austenite stacking fault energy. However, these properties are interrelated and are difficult to isolate for study. As a result, comparisons among various experimental studies are difficult.

Since the martensitic transformation occurs by a shear mechanism, irrespective of the morphology produced, it is especially important to define the effects of austenite SFE and austenite strength on martensite morphology because these properties strongly influence shear processes in the austenite. Austenite stacking fault energy (SFE) controls slip character by controlling the ability of dislocations to cross-slip. The effect of SFE on martensite morphology has been studied by Kelly and Nutting,[14] Breedis,[16] Breedis and Kaufman,[20] and Holden,[21] *et al.* The general trend observed is that the morphology changes from plate to lath to epsilon martensite as the SFE decreases. The effect of austenite strength on martensite morphology has been studied by Davies and Magee,[6,7,12] who found a transition from lath to plate martensite occurred as the austenite yield strength increased.

This paper presents the results of a program designed to study the relative effects of austenite SFE and austenite yield strength at M_S on the morphology of martensite which forms in a series of alloys having a constant carbon content and a constant M_S temperature. By holding these last two variables fixed, one can directly observe the relative roles of slip character and strength in determining the morphology of the transformation product.

ALLOY DESIGN AND PREPARATION

The requirements of this study necessitated the development of alloys covering a wide range of austenite SFE while maintaining carbon content and M_S temperature constant. Alloying for this purpose was based on empirically determined effects of chromium and nickel on austenite SFE as reported in the literature.[13,16,20,22-30] An M_S temperature below room temperature was chosen to permit characterization of austenite substructure by TEM at room temperature. Carbon content was chosen to be 0.3 wt pct. This amount of carbon, by itself, does not favor or preclude the formation of any morphology. Further, this car-

Table I. Compositions of Alloys Used in This Investigation, Wt. Pct

Alloy	Cr	Ni	C	Mn	Al	Si	P	S	N_2
1	0.049	24.87	0.30	0.0043	0.008	0.014	0.006	0.004	0.0022
2	8.90	10.83	0.27	0.004	0.006	0.010	0.005	0.005	0.0043
3	16.43	4.84	0.29	0.003	0.004	0.028	0.008	0.006	0.0027

M. J. CARR is Senior Research Engineer, Rockwell International, Rocky Flats Plant, Golden, CO 80401, J. R. STRIFE is Materials Scientist, Union Carbide Corporation, Central Scientific Laboratory, Tarrytown, NY 10591, G. S. ANSELL is Dean, School of Engineering, Rensselaer Polytechnic Institute, Troy, NY 12180.

Manuscript submitted June 22, 1977.

ISSN 0360-2133/78/0612-0857$00.75/0

bon level permitted reasonable alloy additions of nickel and chromium to satisfy the criteria for SFE and M_S, as well as providing sufficient hardenability.

These alloys were vacuum melted from pure materials in 50-lb heats and hot rolled to about 2.5 mm thick. Prior to testing each alloy was cleaned, homogenized at 1150°C for 48 h under UHP argon in fused quartz ampules, and water quenched. Final treatment of all the alloys consisted of a 50 pct reduction in thickness by rolling, a 30 min austenitizing heat treatment at a temperature chosen to give a grain size of 100 μ, followed by a water quench. The austenitizing temperatures were 1050, 1100, and 1125°C for Alloy 1, 2, and 3 respectively. TEM and optical examination of the as-quenched material showed that all three alloys were single phase in the as-quenched condition.

EXPERIMENTAL PROCEDURES

M_S temperatures were measured by detecting the resistivity change which accompanies the transformation, using a technique described elsewhere.[33]

Austenite yield strength measurements were made by extrapolating data obtained from elevated temperature tensile tests.[32] Sheet tensile specimens were cut parallel to the rolling direction with gage sections measuring 5 by 1 by 0.12 cm. Testing was done on an Instron tester equipped with a heated silicone oil bath. The strain rate for all tests was 4×10^{-4} s^{-1}.

Austenite stacking fault energy was measured at room temperature by the dislocation node method using the theory of Brown and Tholen[34] and following the technique described by Ruff.[25] Measurements of the radius of a circle inscribed in the node were made on at least ten nodes in each alloy and the average taken to represent the SFE.

Optical micrographs were taken to show the gross structure of the transformation product. The fine structure of the morphology of each alloy was characterized on the basis of habit plane and substructure by transmission electron microscopy and electron diffraction analysis. The occurrence of twinning was confirmed by electron diffraction and dark-field techniques.

Foils were prepared for TEM by lap grinding partially transformed (20 pct α') foils down to about 0.13 mm thick. Discs were punched and jet polished at room temperature in 20 pct perchloric acid – 80 pct glacial acetic acid at 10 to 20 V. The foils were examined in a JEOL 100C TEM operated at 100 kV.

The classification of a morphology as lath or plate type was made on the basis of descriptions of these morphologies by Krauss and Marder.[8] Characterization of the morphology was based on microstructural features observed by transmission electron microscopy. Plate martensite is characterized by individual plate-like units, separated by retained austenite, with a habit plane near $(259)_\gamma$ or $(225)_\gamma$ and, in most cases, internal twinning on $(112)_{\alpha'}$. Lath martensite is characterized by parallel and adjacent units with high internal dislocation density. These units form in bands bounded by $(111)_\gamma$ planes and with the long dimension of the laths roughly parallel to $[110]_\gamma$.

RESULTS

M_S Temperatures and σ_{ys} at M_S

The M_S temperatures for Alloys 1, 2, and 3 were -17, -20, and -5°C, respectively. The differences between the M_S temperatures of these alloys are relatively small, and for the purposes of this investigation M_S temperature is considered to be a constant.

Austenite 0.2 pct yield strength *vs* test temperature for all three alloys is plotted in Fig. 1. The extrapolated values of σ_y at M_S are 170, 212, and 263 MPa for Alloys 1, 2, and 3 respectively. The extrapolated value of σ_y at M_S is taken as the measure of austenite strength, since the temperature dependence of σ_y varies from alloy to alloy. The monotonic rise of yield strength with temperature indicates that all the tests were performed above the critical temperature for stress induced martensite formation, so that the observed strength is a true measure of austenite strength. It has been shown[31] that martensite formation prior to or during austenite yielding is indicated by a drop in the measured yield strength relative to a yield strength value extrapolated from higher temperature tests.

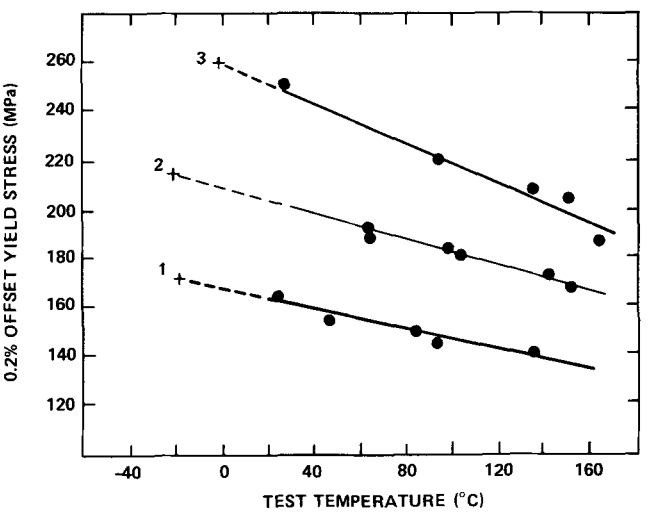

Fig. 1—Yield strength *vs* test temperature for Alloys 1, 2, and 3. The curves are extrapolated to the measured M_S temperatures.

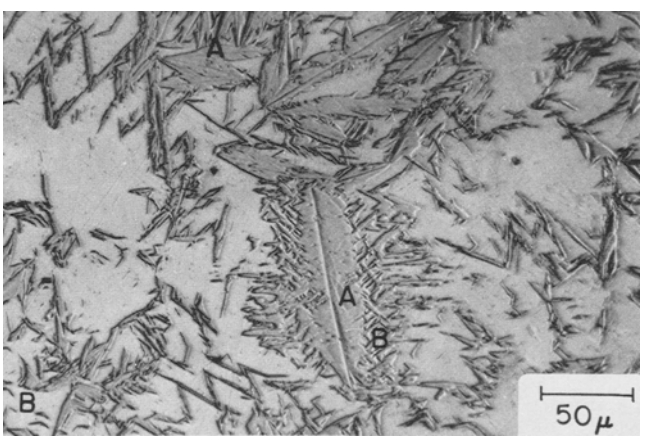

Fig. 2—Optical micrograph of morphology of martensite in Alloy 1.

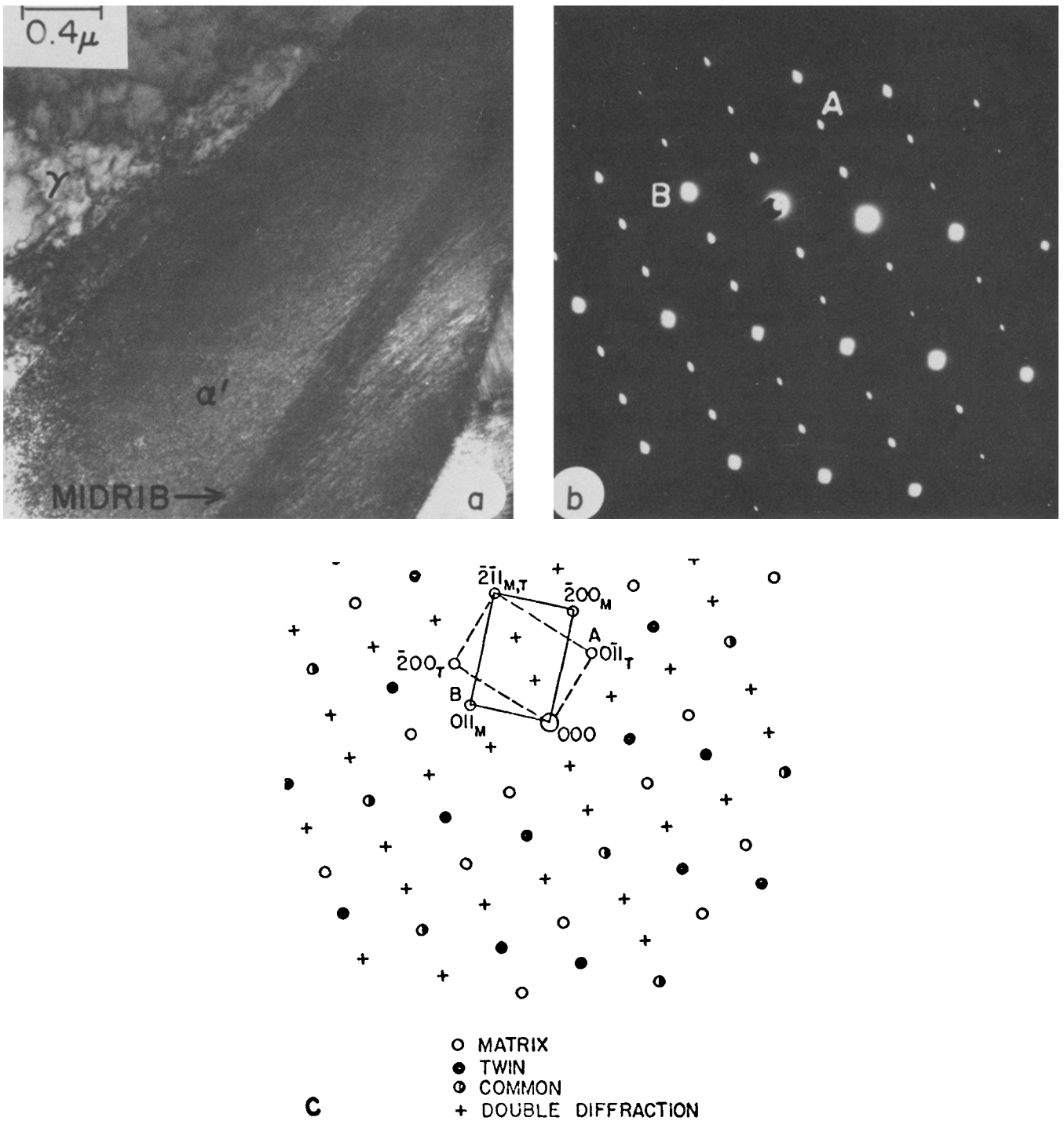

Fig. 3—(*a*) TEM photograph of a midribbed plate in Alloy 1, (*b*) selected area diffraction pattern from the midrib region, (*c*) solution to (*b*), showing twin relationship.

Austenite SFE

The measured austenite SFE for Alloys 2 and 3 were 42 ± 10 Erg/cm^2 and 17 ± 4 erg/cm^2 respectively. No extended nodes of measurable size were found in Alloy 1 so the SFE is assumed to be >50 ergs/cm^2. The sensitivity of this technique varies sharply with the level of SFE being measured. Despite this, it is sufficiently accurate to demonstrate that these alloys represent a wide range in stacking fault energies.

Martensite Morphology

The martensite morphology was different for each of these alloys. Figure 2 is an optical micrograph showing the morphology of Alloy 1. The major fraction of martensite is in the form of large lenticular plates with distinct midribs, often formed in zigzagged arrays (A in Fig. 2). Also evident are smaller chevron shaped units that are clustered near the larger plates (B in Fig. 2). The fine structure of these large

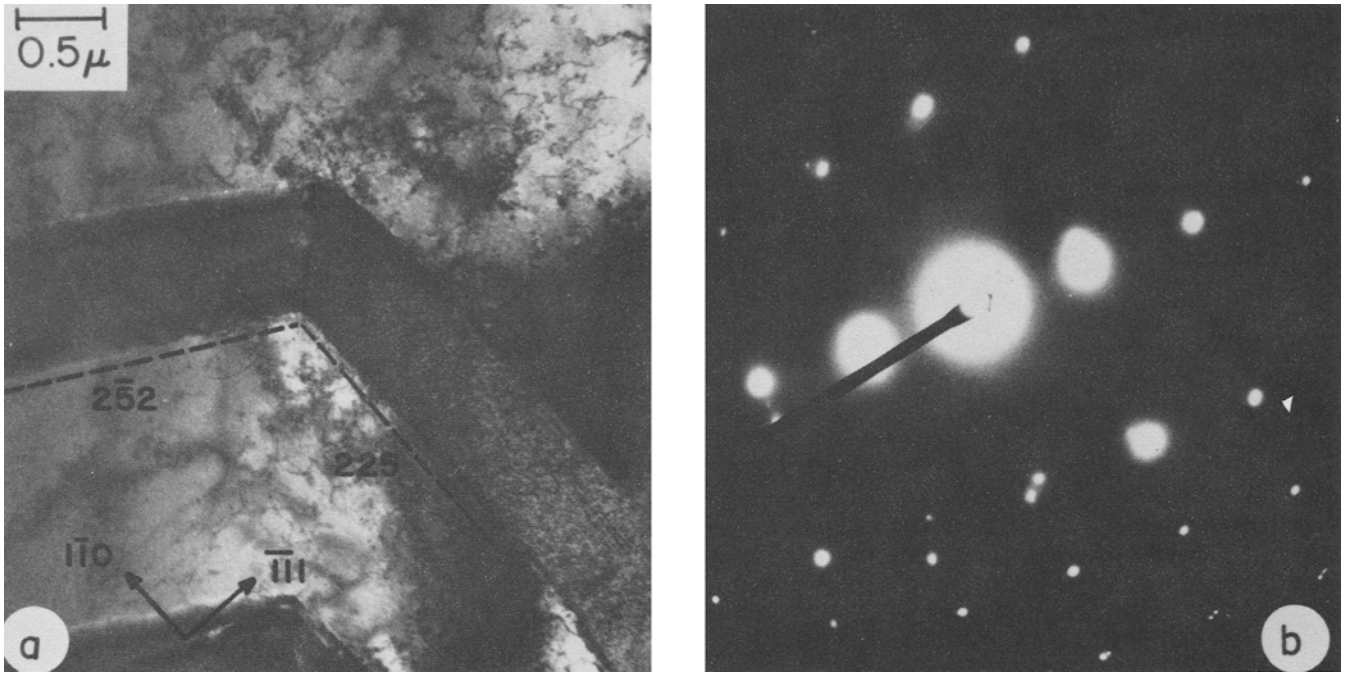

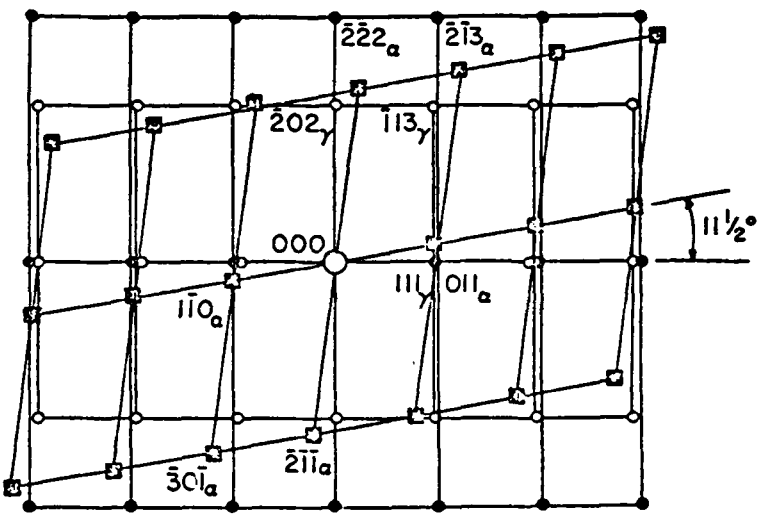

Fig. 4—(*a*) TEM photograph of the apex region of a chevron in Alloy 1, showing $(225)_\alpha$ habit planes, (*b*) selected area diffraction pattern from the apex region, (*c*) solution to (*b*), showing two martensite and one austenite pattern.

plates (A) was studied by TEM. The habit plane of the lenticular plates was near $(259)_\gamma$. As shown in Fig. 3, the midribs of these plates were arrays of fine twins. Except for these twins, the dense substructure was not resolved. The chevron shaped plates were also internally twinned on $(112)_\alpha$ but there was no midrib structure. The habit plane of chevrons was near $(225)_\gamma$, with each arm assuming a different variant of $(225)_\gamma$. A typical chevron is shown in Fig. 4.

Twinning was observed on the $(112)_\alpha$ planes in chevrons, but there was no midrib structure. Finally, chevrons did not form zig-zagged arrays but rather clustered near midribbed plates. It is thought that their formation is assisted by the strain associated with the formation of the large plates. This is supported by the observation that straining the austenite prior to transformation greatly enhances chevron formation.[33]

Alloy 2 also had a plate morphology. As shown in Fig. 5, the martensite took the form of narrow plates running along or out from grain boundaries and twin boundaries. The plates formed at many angles within a grain and a few zig-zagged arrays were found. There were no chevrons as observed in Alloy 1.

TEM confirmed that these units are irregular plates separated by retained austenite. An example of the

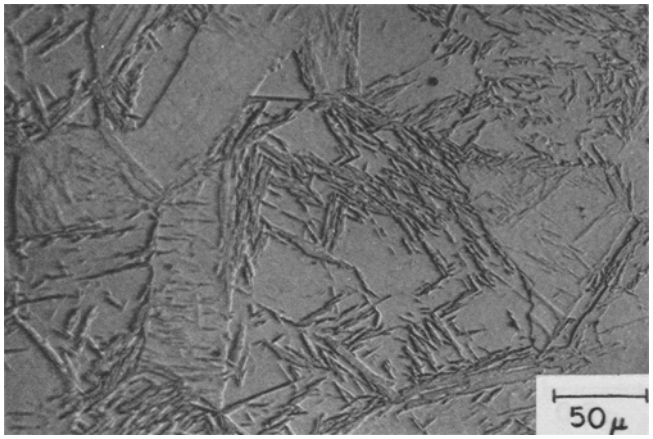

Fig. 5—Optical micrograph of martensite morphology in Alloy 2.

plate structures observed in Alloy 2 is shown in Fig. 6. The martensite habit plane was found to be near $(259)_\gamma$. Twins in these plates were coarser and more irregular than in Alloy 1 and did not form a midrib structure. The twin plane was $(112)_\alpha$.

The martensite morphology observed in Alloy 3 is typical of lath martensite. As shown in Fig. 7, an optical micrograph, parallel bands proceed across grain interiors in only a few growth directions. Observations by TEM, Fig. 8, show that these bands are composed of parallel arrays of heavily dislocated martensite laths. Although it was not possible to determine the habit plane for individual laths, the lath bands were typically delineated by $(111)_\gamma$ planes. Twinning was not observed within individual laths, although adjacent laths were sometimes found to be twin related.

No evidence of epsilon martensite was found either by electron diffraction or X-ray diffraction at room temperature in as-austenized or in partially transformed specimens of Alloy 3. The low SFE of this alloy was expected to promote the formation of epsilon martensite. The absence of epsilon martensite may be an effect of the significant carbon content of this alloy, since carbon has been reported to stabilize against the hcp phase.[24]

Table II. Summary of Morphology, Austenite Strength, and Austenite Stacking Fault Energy

Alloy	SFE, ergs/cm^2	σ at M_s, MPa ksi	Morphology
1	>50	170 (24.7)	(259), (225) plate
2	42	212 (30.7)	(259) plate
3	17	263 (38.2)	lath

DISCUSSION

The data obtained in this investigation are summarized in Table II. The martensite morphology changed from plate to lath as austenite SFE decreased. At the same time, the austenite yield strength at M_s was found to be higher for the alloy with the lath morphology than for the two alloys exhibiting the plate morphology.

In previous investigations concerning the effects of either austenite strength or austenite SFE on martensite morphology, the effects of these variables were studied independently of one another, under experimental conditions too dissimilar to allow comparisons between studies. Breedis[16] investigated a series of Fe-Ni-Cr alloys covering a wide range of SFE and found that a morphology transition from plate to lath occurred as SFE decreased. However, the M_s temperature changes dramatically at the morphology

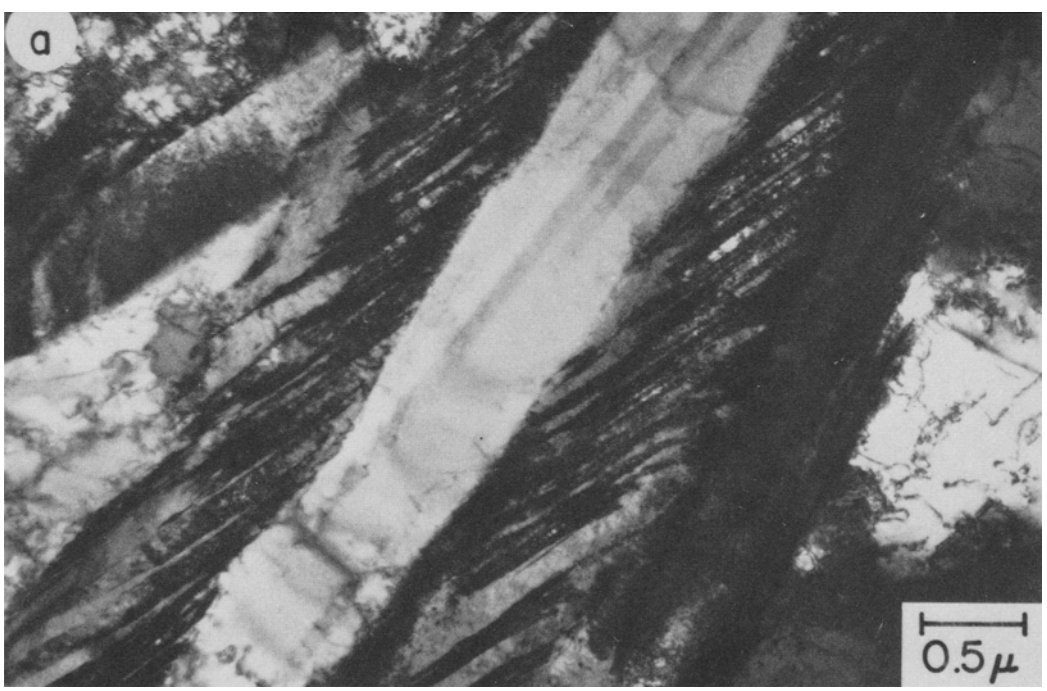

Fig. 6—(*a*) TEM photograph of plates in Alloy 2, showing twinning, (*b*) selected area diffraction pattern of one of the plates, (*c*) solution to (*b*), showing twinning relationships.

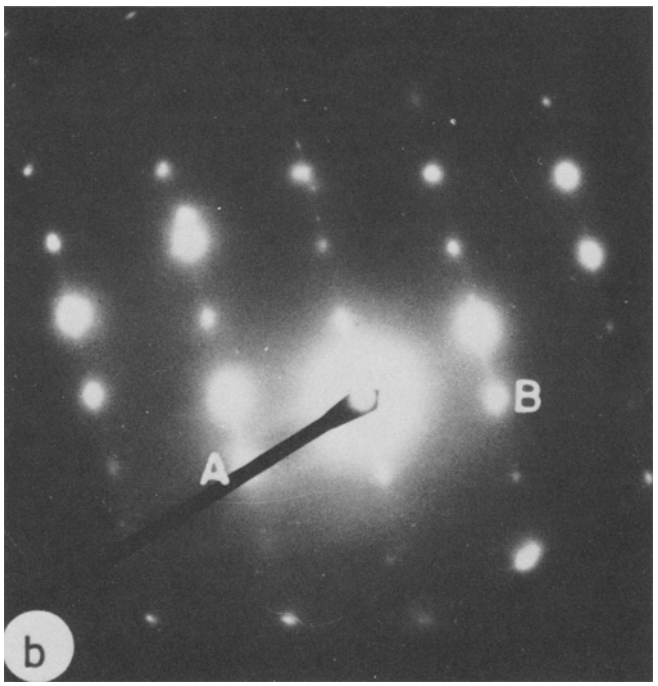

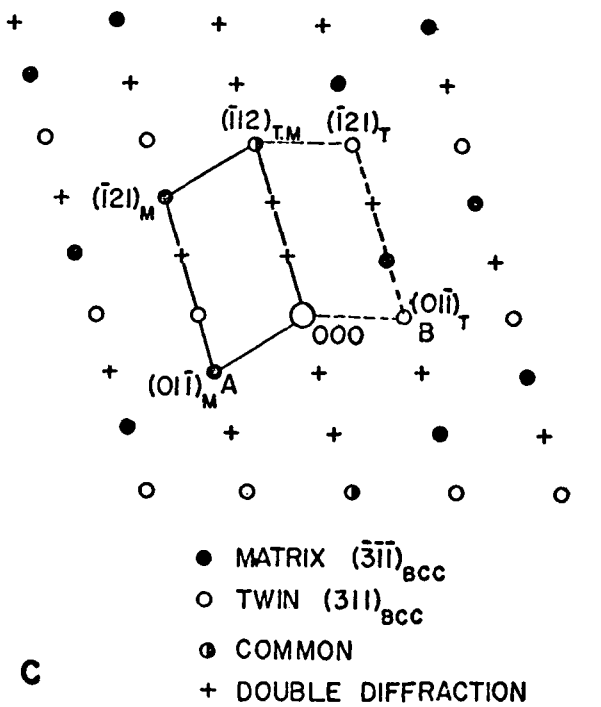

Fig. 6–Continued.

transition, with lath martensite forming at ≥60°C and plate martensite forming near −196°C. Austenite strength was not measured. Holden, *et al*, investigated the structure of as-quenched Fe-Mn alloys and concluded that the morphology was similarly controlled by austenite SFE. Again, the results of that study were obtained at varying M_S temperatures and did not include austenite strength measurements. Kelly[37] studied the effects of austenite stacking fault energy and concluded that lath and plate morphologies correspond to relative minima in the accommodation

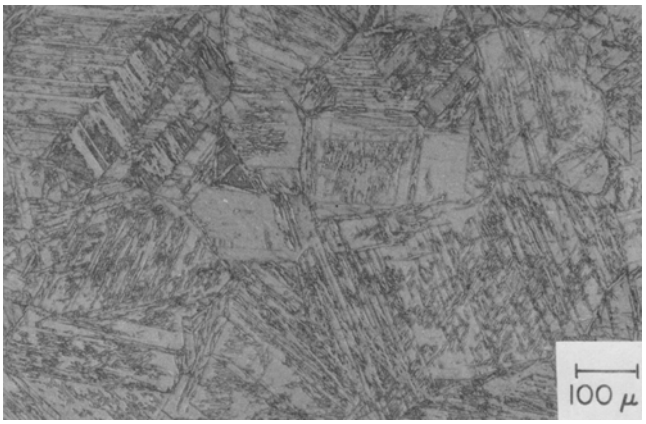

Fig. 7—Optical micrograph of martensite morphology in Alloy 3.

strains which occur during the transformation and are differentiated primarily by the slip system active during the transformation. In a low stacking fault energy material the $(111)[1\bar{2}1]_\gamma$ slip system is active and produces lath martensite. In high SFE materials the multiple slip system $(110)[1\bar{1}0]_\gamma$ is active and produces lath. Recently Khachaturyan,[38] *et al*, have proposed a model of the transformation which describes a mechanism by which austenite stacking fault energy affects the habit plane and thus the morphology of martensite by the production and absorption of stacking faults at the transformation interface.

The effect of as-quenched austenite strength on martensite morphology was studied by Davies and Magee.[6,7] They found that for a wide range of steels the morphology of martensite correlated with the austenite yield strength at M_S. Strong austenites (σy > 207 MPa) produced $(259)_\alpha$ type plate martensite and weak austenites (σy > 103 to 138 MPa) produced lath martensites. Carbon containing alloys with yield strengths between 138 and 207 MPa favored the formation of $(225)_\gamma$ type plate martensites. From these observations, it was postulated that the morphology of martensite which formed in a given alloy was the one which involved the least plastic work for the lattice invariant shear. However, although a wide variety of alloys was studied in that investigation, there were no alloys known to have a low SFE either by measurement or by application of empirical formula[24,39] relating composition to SFE.

This present investigation was undertaken to directly address the question of the relative effectiveness that austenite stacking fault energy and austenite strength have in controlling martensite morphologies. The findings are similar in many respects to those obtained in previous investigations discussed above, and suggest that austenite SFE and austenite yield strength are competing factors in determining martensite morphology.

The two plate forming Alloys (1 and 2) had relatively high austenite stacking fault energies typical of the steels studied by Davies and Magee. The measured austenite yield strengths of Alloys 1 and 2 were 170 and 212 MPa respectively, and they showed a mixed $(225)_\gamma - (259)_\gamma$ type and a $(259)_\gamma$ type morphology, respectively. These data are considered in good agreement with the strength-morphology correlation.

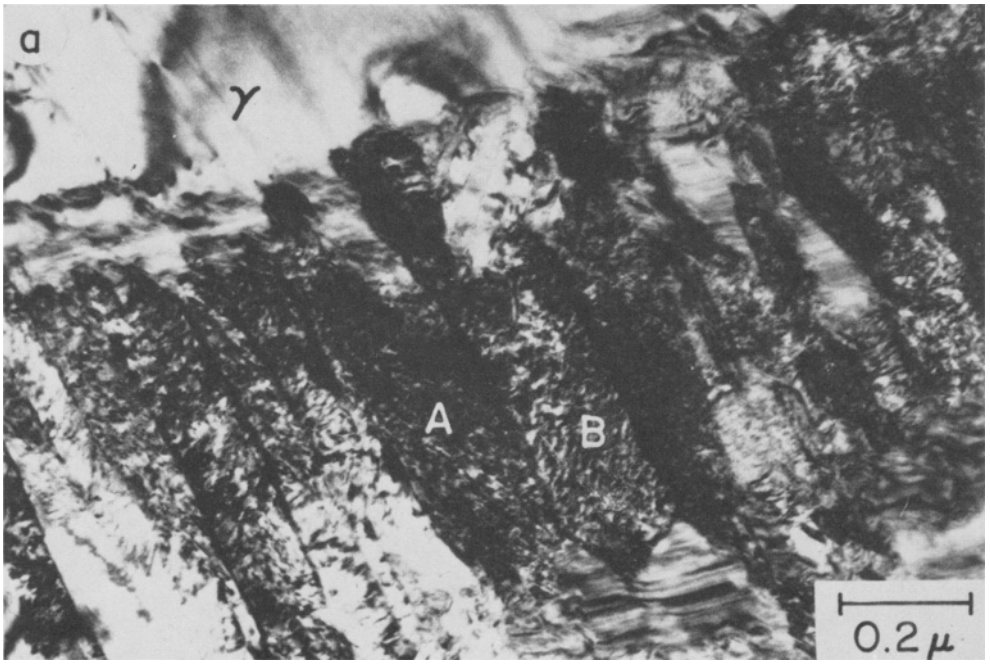

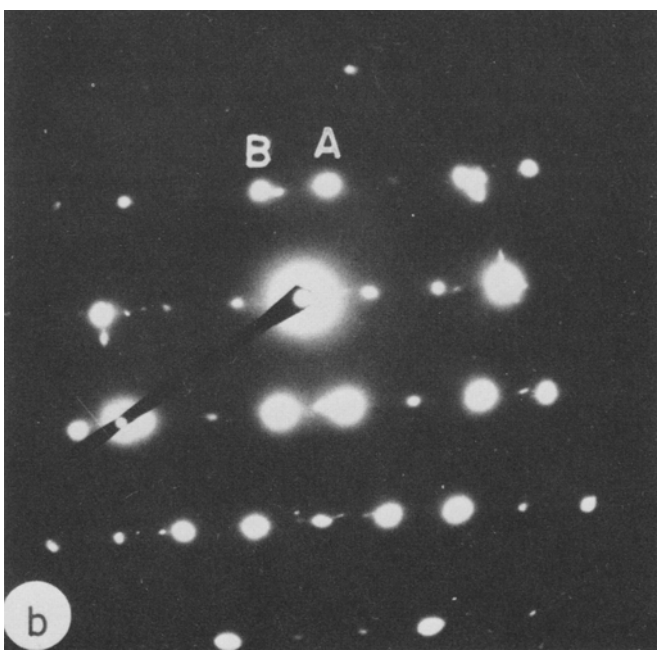

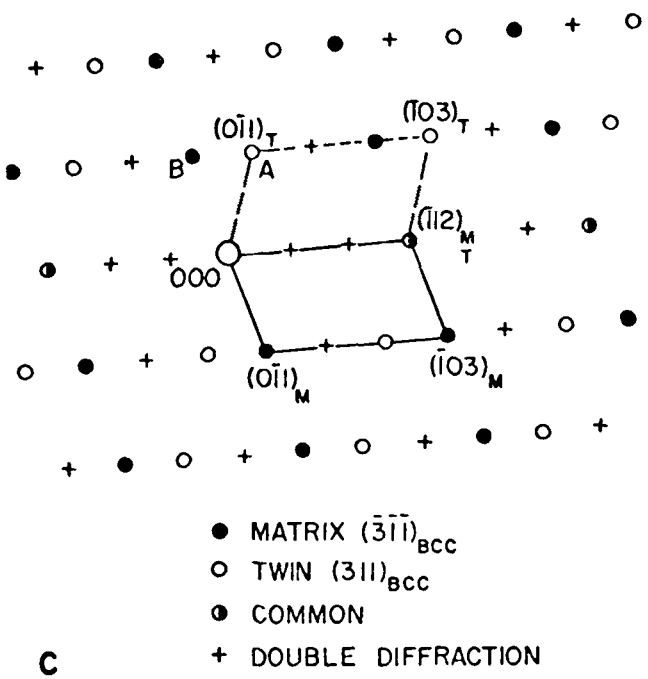

Fig. 8—(*a*) TEM brightfield photograph of a lath band in Alloy 3, (*b*) selected area diffraction pattern from the lath band area containing A and B, (*c*) solution to (*b*), showing twin related $(311)_\alpha$ zones. Laths A and B are twin related.

Alloy 3, however, which had a low SFE, had both a higher strength (263 MPa) and a lath morphology. This level of SFE is typical of the lath forming alloys from previous studies but the strength level is much higher than that previously reported for lath forming alloys. These results are interpreted in the following way. If it is considered that slip is the dominating process for lath formation and that twinning is the dominating process for plate formation, the observed morphology is a result of these two competing processes. The effect of low SFE is to restrict slip to the stacking fault shear system that has been reported[37] to favor lath formation. This forced selection of a slip system promotes lath formation in Alloy 3 at a strength level higher than previously observed for lath forming alloys. A transition to plate martensite with increased strength would still be expected, although at a higher strength in alloys with similarly low SFE.

ACKNOWLEDGMENTS

The authors wist to express their thanks to Allegheny-Ludlum Industries, Inc. for providing the material used in this investigation. Financial support through National Science Foundation Grant DMR73-02411 is appreciated.

REFERENCES

1. P. M. Kelly and J. Nutting: *Proc. Roy. Soc.*, 1960, vol. 259, p. 45.
2. A. R. Marder and G. Krauss: *Trans. ASM*, 1967, vol. 60, p. 651.
3. C. Zener: *Trans. AIME*, 1946, vol. 167, p. 550.
4. J. S. Pascover and S. V. Radcliffe: *Trans. TMS-AIME*, 1968, vol. 242, p. 673.
5. G. Thomas: *Met. Trans.*, 1971, vol. 2, p. 2372.
6. R. G. Davis and C. L. Magee: *Met. Trans.*, 1971, vol. 2, p. 1939.
7. R. G. Davis and C. L. Magee: *Met. Trans.*, 1970, vol. 1, p. 2927.
8. G. Krauss and A. R. Marder: *Met. Trans.*, 1971, vol. 2, p. 2343.
9. C. L. Magee and R. G. Davies: *Acta Met.*, 1971, vol. 19, p. 345.
10. W. S. Owen, G. A. Wilson, and T. Bell: *High Strength Materials*, V. F. Zackey, ed., pp. 167-208, John Wiley & Sons, 1965.
11. D. L. Douglass, G. Thomas, and W. R. Roser: *Corrosion*, 1964, vol. 20, p. 15.
12. R. G. Davies and C. L. Magee: *Proceedings of the 2nd Intl. Conf. on the Strength of Materials*, vol. 3, p. 817, ASM, 1970.
13. J. Nutting: *JISI*, 1969, vol. 6, p. 872.
14. P. M. Kelly and J. Nutting: *JISI*, 1961, vol. 197, p. 199.
15. S. J. Donachie and G. S. Ansell: *Met. Trans. A.*, 1975, vol. 6A, p. 2059.
16. J. F. Breedis: *Trans. TMS-AIME*, 1964, vol. 230, p. 1583.
17. G. S. Ansell, S. J. Donachie, and R. W. Messler: *Met. Trans.*, 1971, vol. 2, p. 2443.
18. S. K. Das and G. Thomas: *Trans. ASM*, 1969, vol. 62, p. 659.
19. S. V. Radcliffe and M. Schatz: *Acta Met.*, 1967, vol. 15, p. 1475.
20. J. F. Breedis and L. Kaufman: *Met. Trans.*, 1971, vol. 2, p. 2359.
21. A. Holden, J. D. Bolton, and E. R. Petty: *JISI*, 1971, vol. 209, p. 721.
22. F. Lecroisey and A. Pineav: *Met. Trans.*, 1972, vol. 3, p. 387.
23. F. Abrassart: *Met. Trans.*, 1973, vol. 4, p. 2205.
24. R. E. Schramm and R. P. Reed: *Met. Trans. A*, 1975, vol. 6A, p. 1324.
25. A. W. Ruff, Jr.: *Met. Trans.*, 1970, vol. 1, p. 2391.
26. R. M. Latanision and A. W. Ruff, Jr.: *Met. Trans.*, 1971, vol. 2, p. 505.
27. R. Fawley, M. A. Quader, and R. A. Dodd: *Trans. TMS-AIME*, 1968, vol. 242, p. 771.
28. D. Dilieu and J. Nutting: *JISI*, Special Report No. 86, 1964, p. 140.
29. R. W. K. Honeycombe, H. J. Harding, and J. J. Irani: *High Strength Materials*, V. Zackey, ed., p. 239, John Wiley and Sons, 1965.
30. W. Charnock and J. Nutting: *Mater. Sci. J.*, 1967, vol. 1, p. 123.
31. D. Bhandarkar, V. F. Zackey, and E. R. Parker: *Met. Trans.*, 1972, vol. 3, p. 2619.
32. E. M. Breinan: Ph.D. Thesis, Rensselaer Polytechnic Institute, 1969.
33. J. R. Strife, M. J. Carr, and G. S. Ansell: *Met. Trans. A*, 1977, vol. 8A, p. 1471.
34. L. M. Brown and A. R. Tholen: *Disc. Faraday Soc.*, 1964, vol. 38, p. 35.
35. M. S. Wechsler, D. S. Lieberman, and T. A. Read: *Trans. AIME*, 1954, vol. 197, p. 1503.
36. J. S. Bowles and J. K. Mackenzie: *Acta Met.*, 1954, vol. 2, p. 129.
37. P. M. Kelly: *JISI*, Special Report No. 86, 1964, p. 146.
38. A. G. Khachaturyan, A. F. Rumynina, and G. V. Kurdjumov: *Trans. JIM*, 1976, vol. 17, p. 273.
39. C. G. Rhodes and A. W. Thompson: *Met. Trans. A.*, 1977, vol. 8A, p. 1901.